

Tunneling Systems in Amorphous Germanium

J. E. Graebner and L. C. Allen

Bell Laboratories, Murray Hill, New Jersey 07974

(Received 16 May 1983)

The thermal conductivity of freestanding films of a -Ge has been measured in the temperature range 0.03–5 K. The results indicate scattering of phonons from tunneling systems, cylindrical voids, and boundaries. The first two mechanisms are correlated with density, the strongest scattering occurring in the samples of lowest density.

PACS numbers: 61.40.Df, 66.70.+f

The amorphous tetrahedral semiconductors a -Ge and a -Si are currently under intense investigation from a fundamental as well as practical point of view. One of the unanswered questions concerns the basic structure of these materials and how it differs from the structure of most glasses. In this Letter we address the question of the existence in these amorphous semiconductors of the two-level tunneling systems^{1,2} (TLS) which nearly universally dominate the properties of glasses at very low temperatures.³ Previous reports^{4–11} on this issue have been contradictory, some claiming the presence and some the absence of tunneling systems. We report measurements of the thermal conductivity of a -Ge films under conditions which overcome problems in previous measurements.⁷ The samples have been carefully characterized and are free standing to avoid difficulties due to the substrate. The data extend over a wide range in temperature, permitting an analysis which takes into account various scattering mechanisms. Evidence for TLS is found in all our films, with the greatest number occurring in the films of lowest average mass density. This correlation with density, observed here for the first time, sheds light on previous contradictions and, more importantly, suggests the location of the tunneling systems. These TLS should also appear in heat-capacity measurements at low temperatures.

The films were deposited at 8–25 Å/sec by evaporation of 99.9999% Ge in an oil-free high-vacuum system capable of maintaining a pressure of $\sim 10^{-8}$ Torr during evaporation. The substrates, located 30 cm from the source, were glass microscope slides coated with ~ 0.1 μm of B_2O_3 as a parting agent. During the Ge deposition the substrates were clamped at their ends against a copper plate controlled at temperature $T_p \sim 100$ C. The films were characterized by infrared and Raman spectroscopy, scanning electron microscopy, and neutron activation analysis. The results of these tests show the films to be typical of unan-

nealed films of a -Ge prepared under high-vacuum conditions.¹² The density (Table I) is computed from the mass and dimensions of the sample. We find that the density is *not* a simple function of T_p ; it depends more on other variables such as evaporation rate and substrate clamping force. Thin-film Manganin heaters and isothermal Au pads¹³ were deposited by evaporation onto the a -Ge films. After electrical and thermal leads were attached, the film was removed from the substrate and mounted by its leads in a ^3He - ^4He dilution refrigerator. The thermal conductivity measurement used a thermal gradient across a narrow region of the Ge film delineated by the heaters and isothermal pads.

The thermal conductivity κ of three representative samples is shown in Fig. 1. The data exhibit a smooth change from a roughly linear variation above 1 K to a T^3 dependence at the lowest temperature. Except for the limiting T^3 rather than T^2 behavior at low temperatures, the magnitude and temperature dependence of the data are roughly similar to those of most glasses cooled from the melt. κ is strongly sample dependent, varying by a factor of ~ 5 at any given temperature, but for all samples it is greater than κ in Ref. 7. In contrast to those results, we find no correlation of κ with sample thickness.

TABLE I. Film characteristics and parameters for samples 1–6 and for the thickest sample (LS) of Ref. 7. Units are the following: thickness t (μm), mass density ρ (g/cm^3), A ($\mu\text{m K}$), B ($\mu\text{m K}^3$), l_b (μm), and l_m (μm).

Sample	t	ρ	A	B	l_b	l_m
1	10.7	5.17	450	721	516	103
2	11.2	4.88	435	234	383	490
3	10.4	4.75	201	206	593	253
4	13.6	4.92	313	210	282	380
5	10.3	4.88	385	211	149	294
6	10.5	4.54	60	170	301	167
LS	5.7	...	250	113	...	163

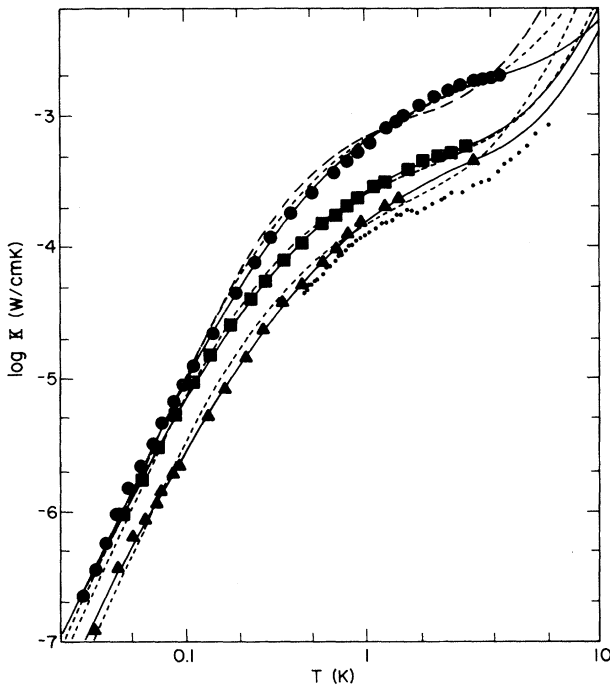


FIG. 1. Thermal conductivity of three representative samples of α -Ge. Circles denote sample 1; squares, sample 3; and triangles, sample 6. The solid lines represent fits of Eq. (1) with the parameters listed in Table I. The dashed lines are fits without TLS as described in the text. The data (solid small dots) for the thickest sample of Ref. 7 are shown for comparison.

Thermal conduction in glasses³ takes place via thermal phonons, and the plateau above 1 K is evidence of a strongly frequency-dependent phonon mean free path $l(\Omega)$, where $\Omega = \hbar\omega/k_B$ and ω is the phonon frequency. We take

$$\kappa(T) = \frac{1}{3}\bar{v} \int_0^{\Omega_D} C(\Omega, T) l(\Omega, T) d\Omega, \quad (1)$$

where C is the Debye heat capacity of the heat carriers (thermal phonons) and \bar{v} is an average phonon velocity. A number of models³ for $l(\Omega)$ have been advanced to yield a rapid variation of l in the appropriate frequency range. To describe the present data, we take the following combination^{13,14} of scattering mechanisms:

$$l(\Omega) = (l_b^{-1} + l_R^{-1} + l_t^{-1})^{-1} + l_m, \quad (2)$$

where we include scattering from the boundaries of the sample (l_b) which we assume to be frequency independent, and Rayleigh scattering from inhomogeneities ($l_R = B/\Omega^m$). Values of $m = 2, 3$, or 4 correspond to Rayleigh scattering from planar, cylindrical, or spherical inhomogeneities, respectively. A minimum value l_m serves as an

upper frequency limit on Rayleigh scattering. l_m also includes complicating effects at the upper end of our temperature range, such as a non-quadratic phonon density of states¹⁵ and phonon-phonon scattering.¹⁶

Scattering from TLS was originally introduced^{1,2} to explain the thermal conductivity typical of most glasses below 1 K. TLS are small groups of atoms capable of tunneling between two different configurations and are thought to be intrinsic to the disordered state. The inverse scattering length due to tunneling may be written¹⁴

$$l_t^{-1} = A^{-1}\Omega \tanh(\Omega/2T) + (4A/\Omega + 4/DT^3)^{-1}. \quad (3)$$

The first term describes resonant scattering, and the second, relaxational. The latter is negligible for the present temperature range but is included for completeness. Figure 1 shows least-squares fits of Eq. (1) to the data. The best fits (solid lines) were obtained by using $m = 3$ and the parameters A, B, l_b , and l_m of Table I.¹⁷ If TLS scattering is *not* included the fits are worse (short-dashed lines). A fit of the data of sample 1 with $m = 4$ and no TLS (long-dashed line) shows that the commonly used Rayleigh scattering contribution is even less adequate. The poorer fits without TLS have $\chi^2/DF > 1$ (where DF is the number of degrees of freedom), compared to $\chi^2/DF < 1$ when TLS are included. In each case, the inclusion of TLS improves (decreases) χ^2/DF by a factor which lies in the range 2–10. A, B, l_b , and l_m each dominate distinct portions of our temperature range and are therefore quite independent of each other. l_m , for example, produces a rise in κ for $T \gtrsim 3$ K and is therefore independent of A , which has a significant effect only for $T \lesssim 2$ K. The reason for the independence of the parameters is the very large change in l (4 orders of magnitude) for the temperature range covered here. The values of A and B that we have fitted to the data of Ref. 7 are consistent with the present results but are statistically meaningless because of the small range of temperature.

The low-temperature T^3 region, in which boundary scattering dominates, yields a mean free path l_b which is 20–50 times the film thickness, implying highly specular reflection.

$m = 3$ corresponds to scattering from cylindrical inhomogeneities with cylinder axes oriented at right angles to the heat flow. Small-angle x-ray scattering¹⁸ from similar thick films of α -Ge indicates cylindrical inhomogeneities roughly 30 Å in diameter and 2000 Å long, with the long axis parallel to the direction of growth. If these re-

gions are voids, the total number of cylinders corresponds to an overall sample density deficit (porosity ν) of (1–2)%. Thus they account for part but not all of the density deficit (up to 30%) in α -Ge. We adapt an expression¹⁹ for Rayleigh scattering from a line of missing atoms in a crystal to obtain

$$l_R \Omega^3 = 4\hbar^3 \nu^3 / 3k_B^3 r d^2, \quad (4)$$

where d is the average diameter of the cylinder. Use of $\nu = 0.01$ yields $l_R \Omega^3 = 360 \mu\text{m}$, in remarkably good agreement with typical values of B in Table I. The criterion for Rayleigh scattering, $\lambda (= 2\pi\nu/\omega) \geq d = 30 \text{ \AA}$, is satisfied for all frequencies up to that corresponding to the transition from $l \approx l_R$ to $l \approx l_m$ ($\lambda \approx 85 \text{ \AA}$ for $l_m \approx 200 \text{ \AA}$ and $B \approx 200 \mu\text{m K}^3$).

The TLS mean free path corresponds to a scattering strength³ $\bar{P}M^2 = \hbar\rho\nu^3/\pi k_B A$, where \bar{P} is the density of states of those TLS which are effective in scattering phonons and M is the phonon matrix element. \bar{P} is a subset of n_0 , the TLS contribution to the specific heat. $\bar{P}M^2$ and the Rayleigh scattering strength, B^{-1} , are shown in Fig. 2 as functions of film density. Both decrease by a large factor as ρ varies from 85% to 97% of the crystalline density. The internal structure of α -Ge is still not fully understood, but it is thought to consist of low-density regions (including the cylinders referred to above) and high- (nearly

crystalline) density regions. The film density then depends upon the fractional volume of each type of region. We interpret the density dependence of $\bar{P}M^2$ as evidence that the TLS are associated with the low-density regions.²⁰ In this picture, the appearance or nonappearance of TLS is at least partially attributable to variations in the density, which was not perceived as an important parameter in previous investigations.^{4–11}

The largest value of $\bar{P}M^2$ in Fig. 2 is just equal to its value in a typical glass, α -SiO₂. If we assume for α -Ge the same fraction of strongly coupled states and a somewhat smaller M (1 eV) compared to α -SiO₂ (1.5 eV), we obtain for our lowest-density film a sufficiently large n_0 to account for the quasilinear heat capacity found recently¹⁰ in α -Ge but attributed instead to paramagnetic spin centers. We predict that careful heat-capacity measurements on well-characterized films of α -Ge will show a substantial tunneling-system contribution that increases with decreasing density.

It is a pleasure to acknowledge many helpful suggestions and a critical reading of the manuscript by B. Golding, as well as useful discussions with J. J. Hauser and B. Bagley. We thank T. Pignataro for developing the lifting technique, C. Doherty for preparing the first film, and K. B. Lyons, D. Aspnes, B. Prescott, J. P. Luongo, D. L. Malm, S. M. Vincent, P. Gallagher, D. Brasen, and J. E. Riley for assistance in analyzing the samples.

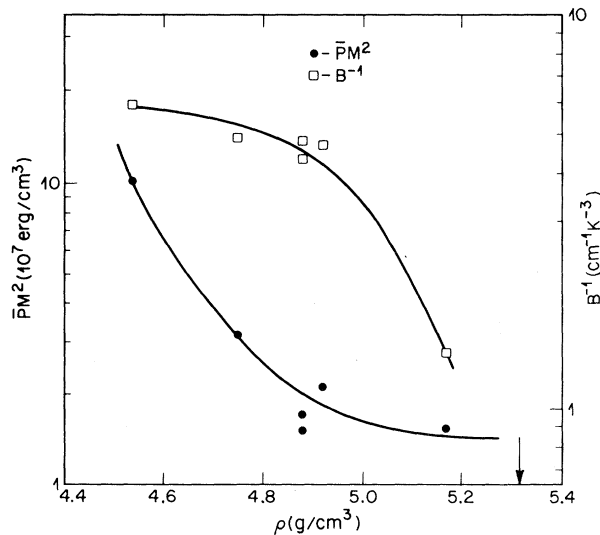


FIG. 2. Scattering strengths $\bar{P}M^2$ due to tunneling systems and B^{-1} due to cylindrical voids, as functions of average mass density. The arrow at 5.32 g/cm^3 indicates the density of crystalline Ge. The lines are intended only as guides for the eye.

¹P. W. Anderson, B. I. Halperin, and C. M. Varma, *Philos. Mag.* **25**, 1 (1972).

²W. A. Phillips, *J. Low Temp. Phys.* **7**, 351 (1972).

³*Amorphous Solids: Low Temperature Properties*, edited by W. A. Phillips (Springer-Verlag, Berlin, 1981).

⁴C. N. King, W. A. Phillips, and J. P. deNeufville, *Phys. Rev. Lett.* **32**, 538 (1974).

⁵A. Cruz-Uribe and J. Trefny, in *Amorphous and Liquid Semiconductors*, edited by W. E. Spear (CICL Univ. of Edinburgh, Edinburgh, 1977), p. 175.

⁶B. Golding, J. E. Graebner, and W. H. Haemmerle, in Ref. 5, p. 367.

⁷H. v. Löhneysen and F. Steglich, *Phys. Rev. Lett.* **39**, 1420 (1977).

⁸M. von Haumer, U. Strom, and S. Hunklinger, *Phys. Rev. Lett.* **44**, 84 (1980).

⁹J. E. Graebner, B. Golding, and T. Pignataro, *Bull. Am. Phys. Soc.* **26**, 418 (1981). This report discusses data from sample No. 1.

¹⁰H. v. Löhneysen and H. J. Schink, Phys. Rev. Lett. **48**, 1121 (1982).

¹¹J. Y. Duquesne and G. Bellessa, J. Phys. C **16**, L65 (1983).

¹²A more complete description of the present work will appear: J. E. Graebner and L. C. Allen, to be published.

¹³M. P. Zaitlin and A. C. Anderson, Phys. Rev. B **12**, 4475 (1975).

¹⁴J. Jäckle, in *The Physics of Non-Crystalline Solids*, edited by G. H. Frischat (Transtech, Rockport, Mass., 1976), p. 568.

¹⁵N. Bilir and W. A. Phillips, Philos. Mag. **32**, 113 (1975).

¹⁶D. P. Jones, N. Thomas, and W. A. Phillips, Philos. Mag. **B38**, 271 (1978).

¹⁷The following constants were used for all samples:

$\bar{v}=3.8\times 10^5$ cm/sec, $\Omega_D=315$ K, and $D=1$ cm⁻¹ K⁻³. The data can be fitted almost as well with $m=4$ if one includes nearly twice as much TLS scattering as with $m=3$. We also note that with $m=4$, the variation of $\overline{PM}^2(\rho)$ is very similar to that shown in Fig. 2 for $m=3$. $m=2$ produces a very poor fit (see Ref. 12).

¹⁸G. S. Cargill, Phys. Rev. Lett. **28**, 1372 (1972).

¹⁹P. G. Klemens, Proc. Phys. Soc. London, Sec. A **68**, 1113 (1955).

²⁰The present data do not allow us to distinguish between *intrinsic* TLS due to Ge-atom defects and *extrinsic* TLS due to, for example, oxygen atoms which are well known to diffuse into low-density films [see, e.g., M. L. Knotek, J. Vac. Sci. Technol. **12**, 117 (1975)]. The latter possibility seems unlikely, however, because of the lack of correlation of A with oxygen content (see Ref. 12).